Journal of Harbin Engineering University
ISSN: 1006-7043

Vol 45 No. 11
November 2024

Design of Thyristor Controlled Series Compensator with Desired Eigen-values in the Sliding Mode

Jaya Prakasa Rao CH[1*], N. D. Sridhar[2] and Ramalla Issac[3]

[1]Research Scholar, Department of Electrical Engineering, Annamalai University, Annamalai Nagar – 608002, Tamil Nadu, India.

[2]Associate Professor Department of Electrical Engineering, Annamalai University, Annamalai Nagar – 608002, Tamil Nadu, India.

[3]Professor, Department of Electrical and Electronics Engineering, Marri Laxman Reddy Institute of Technology and Management Dundigal, Hyderabad – 500 043, Telangana, India.

Abstract

This paper presents an output feedback-based Variable Structure Controller (VSC) designed for a Thyristor Controlled Series Compensator (TCSC), a Flexible AC Transmission System (FACTS) device, to augment the dynamic stability in Electric Power System (EPS). To design the switching surface, the speed deviation, serving as the feedback signal, is connected to the input of the VSC. The objective is to evaluate the effectiveness of the TCSC with VSC in improving stability in a Single Machine Infinite Bus (SMIB) system. The system's dynamic stability is analyzed using eigenvalues and nonlinear time-domain simulations at nominal load conditions. The proposed VSC-based TCSC is compared to TCSC with Feedback control, Power System Stabilizer (PSS) control, and a system without control. Results show that the proposed variable structure feedback-based TCSC controller significantly improves dynamic stability compared to TCSC and PSS control.

Keywords: Thyristor Controlled Series Compensator (TCSC), Dynamic Stability, Variable Structure Control, eigenvalues, and Damping Ratio.

1. INTRODUCTION

Currently, the Electrical Power System (EPS) is under significant strain due to the rising demand for electricity on existing transmission lines and the lack of new transmission infrastructure [1]. For small disturbances, dynamic instability manifests as oscillations with increasing amplitude, typically in the 0.2 to 2.0 Hz range. If appropriate damping is not provided, the system can become unstable. To address these oscillations, a Power System Stabilizer (PSS) is typically applied to the machine's exciter. However, under heavy load conditions, the PSS may not provide adequate damping, leaving the system unstable [2-3]. To overcome this limitation, series FACTS controllers like the TCSC have been employed to improve dynamic stability, offering a more cost- effective solution compared to building new transmission lines [4].

Simplified linear model of PI, provides optimal response at precise operating point. Despite that, concern to varying operating conditions and changes in system parameters, fixed-structure damping controllers tend to deliver suboptimal results. Adaptive controllers have been used to counteract these parameter variations, improving system performance under changing conditions [5]. Despite this, adaptive controllers require real-time system parameter identification, network state monitoring, and rapid calculation of state feedback gains, which makes them more suitable for lower-order, simpler systems, limiting their overall effectiveness. To address Low-Frequency Oscillations (LFOs), intelligent controllers such as Fuzzy Logic Controllers, and Fuzzy PID controllers have been employed. However, these controllers are not well-suited for handling parameter variations and sudden disturbances, which is a significant limitation of this approach [6,7].

To address the limitations mentioned, alternative control strategies have been introduced. A modern feedback nonlinear controller is proposed to enhance network stability and resolve the issues outlined. In cases of sudden disturbances, the Variable Structure Controller

(VSC) shows greater sensitivity to parameter variations. This paper suggests using a sliding mode controller as the control strategy [8]. The mathematical modeling of such controllers proves effective for handling sudden load changes and parameter variations, thereby improving dynamic system stability. Utkin et al. [9] proposed three alternative methods for selecting a switching vector that ensures sliding motion exhibits the desired properties. In the first approach, sliding motion is described with eigenvalues strategically positioned; in the second, the performance index related to the state vector is minimized; and in the third, both the performance index and the equivalent control problem, which focuses on controlling costs in sliding mode, are minimized. From the literature review, it is evident that conventional controllers fail to provide sufficient damping and require more time to achieve steady-state under sudden disturbances. A sliding mode-based VSC has been outlined to address these challenges.

A VSC with a PSS improves damping of critical modes under nominal load, outperforming PI controllers. The switching hyperplane, involving Δδ and Δω, is detailed in the literature [10]. An optimal Variable Structure PSS (VSPSS) has been proposed for single and multi-machine networks, optimizing the switching hyperplane using a quadratic performance index to minimize sliding mode time. However, selecting suitable weight matrices for the performance index is challenging [11,12].

In [13,14], real and reactive powers are the inputs to the VSC based TCSC in unique system. The effectiveness is demonstrated through controller by TCSC using time response and critical modes. This paper primarily focuses on the mathematical analysis, and dynamic modeling of a series FACTS controller. for a small disturbance the eigenvalues are more shifted to left half of S-plane with VSC based TCSC compared to TCSC and also system is subjected to less parameter variations.

In the EPS, the test system's effectiveness is evaluated using an output feedback-based VSC with TCSC. The results show a significant improvement in system damping with the proposed VSC and TCSC, compared to feedback TCSC, PSS, and no controller under nominal load conditions.

2. TEST SYSTEM

The small-signal model of a SMIB system is examined to analyze local LFOs, as illustrated in Fig. 1 [15]. Fig. 2 presents the linearized Heffron-Phillips (HP) model, which is used for stability analysis. In [16], the exciter and machine data are presented for SMIB system.

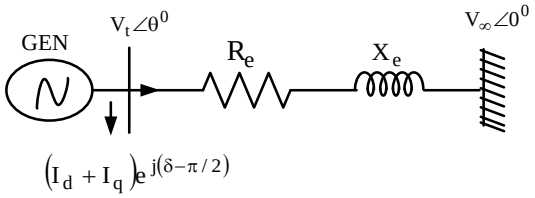

Fig. 1. SMIB test system.

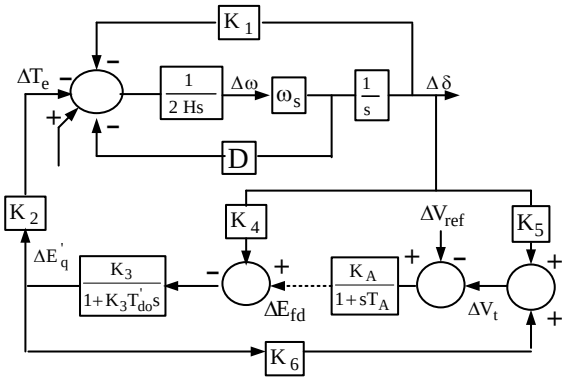

Fig. 2. Linearized HP model for a SMIB system.

Using steady state equations, the initial values of different variables are calculated to calculation of K constants. In Fig.2, the K-constants from K_1 to K_6 as 0.78, 0.63, 0.39, 0.975,0.038 and 0.698.

In EPS, the Differential Algebraic Equations (D.A.E) of EPS is system as [15]:

$$\dot{x} = f(x, y) \quad (1)$$

$$0 = g(x, y) \quad (2)$$

The above equations are linearized to get the eigenvalues from the system matrix.

$$\dot{x} = Ax + Bu \quad (3)$$

$$Y = Cx \quad (4)$$

In this context, 'x', 'u' and 'y' are the vectors corresponds to state, input and output. And also the matrix 'A', 'B and 'C' , belongs to state, control and output.

Where,

The system matrix 'A' ,`B' and 'C' has a dimension of 4×4 , 4×2 and 1×4

$$A=\begin{bmatrix} -0.4304 & -0.1654 & 0 & 0.1695 \\ 0 & 0 & 314 & 0 \\ -0.1000 & -0.2000 & 0 & 0 \\ -1.5e+003 & -77 & 0.001 & -4.995 \end{bmatrix}$$

$$B=\begin{bmatrix} 0 & 0 \\ 0 & 0 \\ 0.2110 & 0 \\ 0 & 2000 \end{bmatrix}$$

$$C=\begin{bmatrix} 0 & 0 & 1 & 0 \end{bmatrix}$$

Additionally, without a controller system transfer function as:

$$\frac{0.211s^3+1.146\,s^2+50.43\,s+1.091\,e-011}{s^4+5.43\,s^3+291.3\,s^2+276.8\,s+11910}$$

For the above transfer function 4 eigenvalues are present. By using equ. (3), A-matrix eigenvalues are calculated and presented in Table-1.

Table 1 Eigenvalues of the SMIB system.

Mode#	Without control	DR(ζ)	Frequency (rad/sec)
$\Lambda_{1,2}$	-2.5872 $\pm$ 14.3260 i	0.1738	15.62
$\Lambda_{3,4}$	**-0.0245 $\pm$ 7.1202 i**	**0.00342**	**7.78**

The DR of the mode $\Lambda_{3,4}$ is 0.00342 and it is small and refer as critical mode. In Table.1 Due to this low damping of the critical mode, the oscillations are rise exponentially and never comes to stable state. The damping controllers PSS and TCSC are placed to the machine to enhance DR of the system.

3. PSS

To eliminate the negative damping, PSS produces the supplementary damping to the rotor excitation. In Fig.3, three blocks are present. The gain block produces the damping to the critical mode $\Lambda_{3,4}$. The block 2 is omitted and in block 3 , the time constants T_1 and T_2 produces the damping torque to the modes.

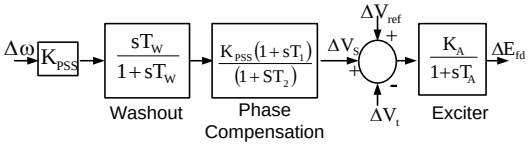

Fig. 3. Exciter with PSS

The I/P and O/P of PSS are the speed deviation from synchronous speed, denoted as $\Delta\omega_m$, and the voltage deviation, represented as ΔV_S. At the summing point, ΔV_S is combined with ΔV_{ref} and ΔV_t to help reduce oscillations within the network [2, 14]. The equations for the system matrix (A_{SYS}) for the system incorporating PSS, are detailed in [16].

Table 2 Eigenvalues of the network with PSS.

Mode ≠	System with PSS	DR (ζ)	Frequency (rad/sec)
$\Lambda_{1,2}$	-2.2125 $\pm$ 15.48 i	0.1825	15.6
$\Lambda_{3,4}$	**-0.3792 $\pm$ 7.755 i**	**0.0501**	**7.57**
$\Lambda_{5,6}$	-10.4290	1.0	10.40

The input to the PSS is$\Delta\omega_m$, and ΔV_S is the output of the PSS. To mitigate the oscillations, at the summing point ΔV_S , ΔV_t and ΔV_{ref} are combine [2]. After, the insertion of PSS, the system matrixA_{SYS}, B and C equations are presented in [16].

Placing of PSS in the system,the DR of the $\Lambda_{3,4}$ is improved from 0.00342 to 0.0501in Table-2. The DR of the mode improves, but further enhancement can be achieved by placing TCSC to the network.

4. DESIGN OF TCSC

The TCSC controller is placed in series with the line of Fig.(1). By vary, firing angle α, series reactance in the transmission line vary. Fig.4, represents the damping controller of TCSC.

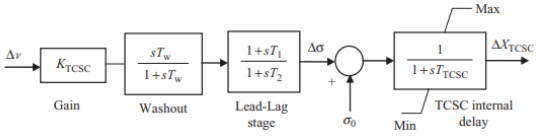

Fig. 4. TCSC damping controller.

In Fig. 4, three blocks represent a PSS damping controller, as described in [13]. By adjusting the firing angle, ∝, the system's net reactance changes, enhancing damping. With the TCSC inserted, the two state variables, Δ∝ and ΔX_{TCSC}, are summing to the generator in Equation (3), resulting in two additional eigenvalues in the system matrix. TCSC values are provided in [15], and the K-constants associated with TCSC are given in [16].

$K_3=0.5313$, $K_4=0.4952$, $K_1=0.9751$, $K_2=0.5668$, $K_5=0.0374$, and $K_6=0.8231$

$$X=\begin{bmatrix}\Delta E_q' & \Delta\delta & \Delta\omega\Delta E_{fd} & \Delta\propto & \Delta X_{TCSC}\end{bmatrix} \quad (5)$$

$$A\_TCSC = \begin{bmatrix} -0.302 & -0.1 & 0 & 0.5 & 0 & 0 \\ 0 & 0 & 314 & 0 & 1 & 0 \\ -0.1 & -0.21 & 0 & 0 & 0.62 & 0 \\ -1653.3 & -75.7 & 0 & -5.0 & 2003 & 0 \\ 1.520 & 2.65 & -43 & 0 & -20.8 & 0 \\ 0 & 0 & 0 & 0 & 0 & 0 \end{bmatrix}$$

$$B\_TCSC = \begin{bmatrix} 0 & 0 \\ 0 & 0 \\ 0.22 & 0 \\ 0 & 2005 \\ -4.35 & 0 \\ 0 & 0 \end{bmatrix}$$

$$C\_TCSC = \begin{bmatrix} 0 & 0 & 3 & 0 & 0 & 0 \end{bmatrix}$$

With TCSC controller, the system transfer function is

$$\frac{0.212s^5 + 3.34s^4 + 71.58s^3 + 567.9s + 25.78s}{s^6 + 27.18s^5 + 463.2s^4 + 6075s^3 + 18270s^2 + 11780s + 4287}$$

For the above transfer function, 6 eigenvalues are present. Table. 3, represents test system eigenvalues with TCSC. The mode $\boldsymbol{\Lambda_{3,4}}$ DR improved from 0.0501 to 0.2046, respectively.

Table 3 Eigenvalues of test system with TCSC.

Mode ≠	System with TCSC	DR (ζ)	Frequency (rad/sec)
$\Lambda_{1,2}$	-3.2100 ± 16.10 i	0.1960	16.400
$\Lambda_{3,4}$	**-0.9710 ± 4.63 i**	**0.2046**	**4.73**
$\Lambda_{5,6}$	-0.040, -17.80	1.0, 1.0	0.040, 17.80

5. VARIABLE STRUCTURE SYSTEM (VSS)

To enhance dynamic stability, the control signal 'u' in Equation 3 significantly improves the damping effect. This improvement is notable across various operating points.

For linear regulator state feedback controller is defined as follows:

$$U = K^T.X \quad (6)$$

In the above Equ. (6), K is the gain matrix of the state feedback and it is selected through the method of quadratic minimisation approach.

At switching hyperplane, a change of structure will take place and called as switching function

$$S = G^T X = 0 \quad (7)$$

In equ. (7), $'G'$, depicts the constant vector.

The conditions for sliding modes states appears on the sliding surface are $Lt_{S\to 0^-}\dot{S} > 0$ and $Lt_{S\to 0^+}\dot{S} < 0$

The above conditions are enough to ensure the existence of a sliding mode.

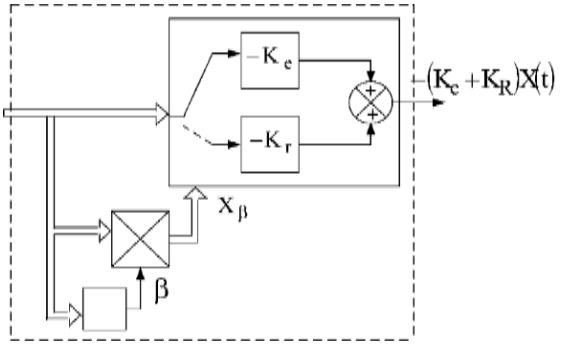

Fig. 5. Variable Structure with TCSC.

In this Fig.5, two stages are present. The first stage is the control law (K_e), to place the states on the sliding surface (S) and second stage $(K_r)$is to move the states to the sliding surface [18-20].

6. DESIGN OF TCSC WITH VSC

To improve dynamic stability, the TCSC is placed in series with a transmission line. By adjusting the firing angle of the thyristors, the TCSC can smoothly and rapidly alter its apparent reactance [21].

The transformation matrix M is selected such that the first (n−1) rows are orthogonal to vector b, while the product of the n^{th} row of M and b is nonzero. Therefore, M is defined as...

$$M = \begin{bmatrix} 1 & 0 & 0 & 0 & 0 & 0 \\ 0 & 1 & 0 & 0 & 0 & 0 \\ 0 & 0 & 1 & 0 & 0 & 0 \\ 0 & 0 & 0 & 1 & 0 & 0 \\ 0 & 0 & 0 & 0 & 0 & 1 \\ 0 & 0 & 0 & 0 & 1 & 0 \end{bmatrix}$$

The matrix 'M' is the order of 6×6

The matrices A_{11}, A_{12}, A_{21} and A_{22} of the matrix $MA_{SVeC}M^{-1}$ for the system investigated, are:

$\tilde{A}$ is the order of 6×6

$\tilde{A}_{11} = (n_i - m_i)\times(n_i - m_i)$ and it is the order of 4×4

$$\tilde{A}_{11} = \begin{bmatrix} -0.3 & -0.1 & 0 & 0.2 \\ 0 & 0 & 314 & 0 \\ -0.1 & -0.1 & 0 & 0 \\ -1646 & -74.7 & 0 & -5 \end{bmatrix}$$

$\tilde{A}_{12} = (n_i - m_i) \times m_i$ and it is the order of 4×2

$$\tilde{A}_{12} = \begin{bmatrix} 0 & 0 \\ 0 & 0 \\ 0 & 0.5 \\ 0 & 2000 \end{bmatrix}$$

$\tilde{A}_{21} = m_i \times (n_i - m_i)$ and it is the order of 2×4

$$\tilde{A}_{21} = \begin{bmatrix} 0 & 0 & 0 & 0 \\ 1.5 & 2.5 & -40 & 0 \end{bmatrix}$$

$\tilde{A}_{22} = m_i \times m_i$ and it is the order of 2×2

$$\tilde{A}_{22} = \begin{bmatrix} 0 & 0 \\ 0 & -20.8 \end{bmatrix}$$

CALCULATE 'P' MATRIX: P is the solution of Riccati equation

$$P\tilde{A}_S + \tilde{A}_S^T P - P\tilde{B}_S \tilde{R}_S^{-1} \tilde{B}_S^T P + \tilde{Q}_S = 0$$

$$\tilde{P}_{SMC} = \begin{bmatrix} 41.8 & -8.5 & 136.7 & -0.0 \\ -8.5 & 2.4 & 2.5 & -0.0 \\ 136.7 & 2.5 & 9730.7 & -2.4 \\ -0.00 & -0.0 & -2.4 & 0.0 \end{bmatrix}$$

$$\tilde{S}_{SMC} \begin{bmatrix} -1999.8 \\ -0.4 + i5.1 \\ -0.4 - i5.1 \\ -1.0 \end{bmatrix}$$

$$\tilde{K}_{SMC} = \begin{bmatrix} 0 & 0 & 0 & 0 \\ 7.0376 & -1.5559 & 39.4342 & 0.9883 \end{bmatrix}$$

Sliding surface S or h:

This switching sliding surface is a function of portioned $\tilde{A}, \tilde{Q}$ matrices and transformed matrix (M) .

$$S = \left[\tilde{Q}_{22}^{-1}\left(\tilde{A}_{12}^{'}.P_{SMC} + \tilde{Q}_{12}^{'}\right) \quad I\right] * M$$

$$h_{SMC} = \begin{bmatrix} 0 & 0 & 0 & 0 & 1.0 & 1.0 \\ 7.0376 & -1.5559 & 39.4342 & 0.9883 & 1.00 & 1.0 \end{bmatrix}$$

$$K_{eSMC} = \left(H_{SMC}.\tilde{B}\right)^{-1}.H.\tilde{A}$$

$$K_{eSMC} = \begin{bmatrix} -0.3437 & -0.5912 & 9.4800 & 0 & 0.0095 & 4.9447 \\ -0.8213 & -0.0377 & -0.2871 & -0.0019 & -0.00 & 0.9900 \end{bmatrix}$$

$K_{rSMC} = \left(H_{SMC}.\tilde{B}\right)^{-1}.H..\delta$, where δ is the sliding margin and it is assumed to be 0.85

$$K_r = \begin{bmatrix} 0 & 0 & 0 & 0 & -0.2133 & -0.2133 \\ 0.0032 & -0.0007 & 0.0180 & 0.0005 & 0.0009 & 0.0009 \end{bmatrix}$$

Linear feedback control law for VSS is given by

$u = -KX = -(K_e + K_r)X = -(K_{eSMC} + K_{rSMC})x =$

$K_{SMC} = (K_{eSMC} + K_{rSMC})$

$$K_{SMC} = \begin{bmatrix} 0.3437 & 0.5912 & -9.4800 & 0 & 0.2038 & -4.7314 \\ 0.8211 & 0.0384 & 0.2691 & 0.0014 & -0.0009 & -0.9909 \end{bmatrix}$$

λ_S (Sliding eigenvalues) = $\text{eig}\left(\tilde{A} - \tilde{B}.K_{SMC}\right)$

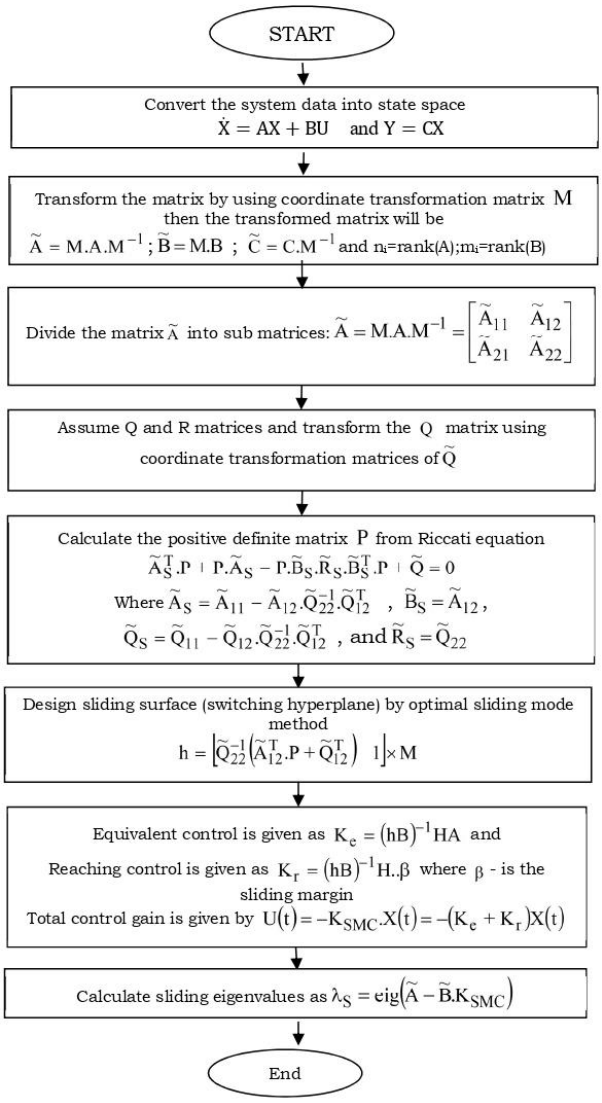

Fig. 6. Flowchart for VSC with TCSC in a system

Table 4 Eigenvalues with VSC based TCSC

Mode ≠	System with PSS	DR (ζ)	Frequency (rad/sec)
$\Lambda_{1,2}$	-4.8015 ± 22.376 i	0.2105	22.900
$\Lambda_{3,4}$	**-1.3242 ± 4.6567 i**	**0.274**	**4.84**
$\Lambda_{5,6}$	-34.7485, -0.0400	1,1	34.7485, 0.0400

Table – 4, presents the eigenvalues of the network with VSC based TCSC and order of A_{sys} is 6 , result six modes and eigenvalues are present. All moved to left of S-plane, indicating that the network is dynamically stable. It is observed that the eigenvalue of the critical mode (-1.3242 ± 4.6567 i) is more shifted to imaginary axis of s-plane result the damping is enhanced to 0.274 from

0.2050 Hence, the system is more dynamically stable with sliding mode compares to without control.

7. RESULTS AND DISCUSSIONS

To analyse the performance of the proposed VSC with TCSC, the system is subjected to a small disturbance. Fig.7, presents the nominal operating dynamic response [15,21].

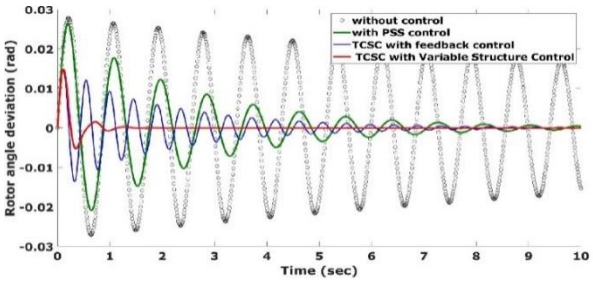

Fig.7. Rotor angle deviation '$\Delta\delta$' (rad) of the test system.

Fig. 7, illustrates the comparative dynamic stability of system under four scenarios: without damping control, with PSS, with feedback TCSC, and with VSC based TCSC. These comparisons are conducted to evaluate the system's performance over a duration of 10 seconds. whereas '$\Delta\delta$' is the rotor angle of machine synchronous machine, respectively.

The system is unstable without control, attributed to the mode, $\Lambda_{3,4}$ is −0.024+7.02 i, in Table 1, which exhibits poor DR. After a Power System Stabilizer (PSS) is placed in the exciter of the system, the $\Lambda_{3,4}$ improves to −0.3792+7.755i (Table 2), shifting from its previous value of −0.0234+7.03i. This results in a damping improvement to 0.047, which is further enhanced by TCSC.

With TCSC, the $\Lambda_{3,4}$ has moved from −0.38 ± 7.76i to −0.98 ± 4.63i (Table 3), resulting in improved system damping. In fact, the oscillation mode has stabilized, and both the settling time (t_s)and peak overshoot ($\%M_p$) have been less comparison to the scenarios of afore said controller. Thus, the system with TCSC has been effectively stabilized.

When comparing the VSC with the TCSC as a feedback controller, the mode $\Lambda_{3,4}$ shifts from −0.98 ± 4.63i (Table 3) to −1.325 ±4.657 i(Table 4). Results in greater enhancement of damping and more stable with VSC.

In Fig. 7, the settling times (t_s), for the oscillations of '$\Delta\delta$' is t_s =123.29 s, 10.9 s, 4.4 s, and 3.9 s, respectively, for the scenarios without control, with PSS, with TCSC, and with VSC-based TCSC. The overshoot percentages ($\%M_P$) are 1.0095%, 0.8523%, 0.4563%, and 0.2683% for the same conditions.

From Fig. 7, it can be observed that the system with the VSC exhibits the smallest amplitudes, shortest settling time, and reduced overshoot and undershoot, along with a quick recovery to pre-disturbance conditions.

The incorporation of sliding mode control to address the system's nonlinearity is a significant advantage of this controller. However, a major limitation of the controller is its difficulty in application to higher-order systems, primarily due to challenges in measuring system states. These issues regarding the unavailability of system variables can be mitigated by using an observer-based sliding mode controller.

8. CONCLUSION

An output feedback based VSC with TCSC controller has been developed to enhance the stability in EPS. A key advantage of this controller is that it utilizes only physically measurable speed deviation signals as inputs, facilitating easier practical implementation. Furthermore, when the system in sliding mode, its dynamic performance shows a notable insensitivity to fluctuations for various operating and parameters of the plant. Simulation results demonstrate that the variable structure TCSC controller effectively improves the dynamic stability in EPS.

REFERENCES

[1] Anderson, P.M. Fouad, A.A (2003) Power System Control and Stability. John Wiley & Sons, India.

[2] Kundur, P, Balu, N J and Lauby M G (1994) Power system stability and control. McGraw-hill, New York.

[3] Amin Safari, Hossein Shayeghi, Heidar Ali Shayanfar (2016) Coordinated control of pulse width modulation-based AC link series compensator and power system stabilizers. Electrical Power and Energy systems, 83: 117-123. https://doi.org/10.1016/j.ijepes.2016.03.042.

[4] Hingorani, N H, and Gyugyi. L(2000) Understanding FACTS: Concepts and Technology of Flexible AC Transmission System. Wiley- IEEE press, India.

[5] A. Ghosh, G Ledwich, O.P.Malik and G.S.Hope, (1984) Power System Stabilizer based on adaptive control techniques :IEEE Transactions on power Apparatus and Systems, 103: 1983-1989. DOI: 10.1109/TPAS.1984.318503.

[6] H. Shayeghi, H.A. Shayanfar., and Jalli (2009) Load Frequency Control Strategies : A state of the art Survey for the Researcher: Energy Conversion and Management. 50:344-353. https://doi.org/10.1016/j.enconman.2008.09.014.

[7] Ibraheem, Prabhat Kumar and Dwaraka P.Kothari (2005) Recent Philosphies of Automatic Generation Control Startegies in Power System. IEEE Transactions on Power Systems.20:346-357. DOI: 10.1109/TPWRS.2004.840438.

[8] M.L. Kothari, J. Nanda, and K. Bhattacharya (1993) Design of variable structure power system stabilisers with desired eigenvalues in the sliding mode. IEE proceedings Generation, transmission and distribution 140:263-267. DOI: 10.1049/ip-c.1993.0039.

[9] Utkin .I, and Yang,K.D (1978) Methods for constructing discontinuity planes in multidimensional variable structure systems: Automation and Remote control, 39: 1466-1470. DOI: 10.1016/0005-1098(78)90071-7. https://doi.org/10.1016/0378-7796(83)90014 -7.

[10] G. Venkataramanan and B.K. Johnson, (2002) Pulse width modulated series compensator," IEEE Proc. Gen. Trans and Dist, 149: 71-75, DOI: 10.1049/ip-gtd:20020004.

[11] CHAN, W.C., and HSU, Y.Y (1983) An optimal variable structure stabilizer for power system stabilization: IEEE Trans. Power apparatus and systems, 102: 1738-1746. DOI: 10.1109/TPAS.1983.317916.

[12] M.L. Kothari and CHAN (1983) Stabilization of power systems using a variable structure stabilizer. Electric Power Systems Research 6:129-139.

[13] Tain-Syh Luor, Yuan-Yih Hsu (1998) Design of an output feedback varaible structure thyristor-controlled series compensator for improving power system stability: Electrical Power Systems Research, 47: 71-77. https://doi.org/10.1016/S0378-7796(98)00049-2.

[14] G. Venkataraman an and B.K. Johnson, (2002) Pulse width modulated series compensator," IEEE Proc. Gen. Trans and Dist, 149: 71-75, DOI: 10.1049/ip-gtd:20020004.

[15] Debasish Mondal, Abhijit Chakrabarti and Aparajita Sengupta(2014) Power System Small Signal Stability and Control. Academic Press, Elsevier,India.

[16] K Himaja, T.S Surendra and S. Tara Kalyani (2021) Dynamic Stability Analysis of a SMIB system with PSS and LQR optimal control: Proc. ICIPTM, Noida, India. DOI**:** 10.1109/ICIPTM52218.2021.9388318.

[17] Y. Welhazi, Tawfik Guesmi, I. B. Jaoued and Hsan Haj Abdallah, "Power system stability enhancementusing FACTS controllers in multimachine power systems", Journal of Electrical Systems, vol. 10, no. 3, pp. 276-291, 2014.

[18] Kai Liao, Zhengyou He, Yan Xu, Guo Chen, Zhao Yang Dong and Kit Po Wong (2017)A sliding mode based damping control of DFIG for interarea power oscillations: IEEE Transactions on sustainable Energy,8:258-267,DOI: 10.1109/TSTE.2016.2597306 .

[19] Lionel Leory Sonfack, Godpromesse Kenne and Andrew Muluh Fombu (2018) A new Static Synchronous Series Compensator control strategy based on SMIB system RBF Neuro-Sliding Mode technique for power flow control and DC voltage regulation: Electric Power Components and Systems, 46: 456-471. https://doi.org/10.1080/15325008.2018.1445795.

[20] F.L. Lewis, D. Vrable and V. L. Syrmos "Optimal control",(book) John Wiley. 1986.

[21] M. Athans and P. Falb, "Optimal control: an introduction to the theory and its Application" (book) McGraw-Hill, 1966.